

# Evidence for Water in the Rocky Debris of a Disrupted Extrasolar Minor Planet

J. Farihi<sup>1,4\*</sup>, B. T. Gänsicke<sup>2</sup>, D. Koester<sup>3</sup>

<sup>1</sup>Institute of Astronomy, University of Cambridge, Cambridge CB3 0HA, UK

<sup>2</sup>Department of Physics, University of Warwick, Coventry CV5 7AL, UK

<sup>3</sup>Institut für Theoretische Physik und Astrophysik, University of Kiel, 24098 Kiel, Germany

<sup>4</sup>STFC Ernest Rutherford Fellow

\*To whom correspondence should be addressed; E-mail: jfarihi@ast.cam.ac.uk

**The existence of water in extrasolar planetary systems is of great interest as it constrains the potential for habitable planets and life. Here, we report the identification of a circumstellar disk that resulted from the destruction of a water-rich and rocky, extrasolar minor planet. The parent body formed and evolved around a star somewhat more massive than the Sun, and the debris now closely orbits the white dwarf remnant of the star. The stellar atmosphere is polluted with metals accreted from the disk, including oxygen in excess of that expected for oxide minerals, indicating the parent body was originally composed of 26% water by mass. This finding demonstrates that water-bearing planetesimals exist around A- and F-type stars that end their lives as white dwarfs.**

The enormous recent progress in the discovery of exoplanetary systems provides a growing understanding of their frequency and nature, but is still limited in many respects. There is now

observational evidence of rocky exoplanets (2, 1), yet transit depth plus radial velocity amplitude provide planet mass and radius (and hence density), while the bulk composition remains degenerate and model dependent. Transit spectroscopy offers some information on giant exoplanet atmospheres (3), and planetesimal debris disks often reveal the signature of emitting dust and gas species (4), yet both techniques only scratch the surface of planets, asteroids, and comets. Interestingly, white dwarfs – the Earth-sized embers of stars like the Sun – offer a unique window onto terrestrial exoplanetary systems: these stellar remnants can distill entire planetesimals into their constituent elements, thus providing the bulk chemical composition for the building blocks of solid exoplanets.

Owing to high surface gravities, any atmospheric heavy elements sink rapidly as white dwarfs cool below 25 000 K (5), leaving behind only hydrogen and helium in their outermost layers, a prediction that is corroborated by observation (6). Those white dwarfs with rocky planetary system remnants can become contaminated by the accretion of small, but spectroscopically detectable, amounts of metals.<sup>1</sup> Heavy element absorption lines in cool white dwarfs are a telltale of external pollution that often imply either ongoing mass accretion rates above  $10^8 \text{ g s}^{-1}$  (7), or large asteroid-sized masses of metals within the convection zone of the star (8).

In recent years, metal-rich dust (9, 10) and gas (11) disks, likely produced by the tidal disruption of a large asteroid (12), have been observed to be closely orbiting 30 cool white dwarfs [e.g. (13, 15, 16, 14, 17, 18)] and provide a ready explanation for the metal absorption features seen in their atmospheres (19). The circumstellar material being gradually accreted by the white dwarf can be directly observed in the stellar photosphere to reveal its elemental abundances (20). These planetary system remnants offer empirical insight into the assembly and chemistry of terrestrial exoplanets that is unavailable for any exoplanet orbiting a main-sequence star.

---

<sup>1</sup>Astronomers use the term ‘metal’ when referring to elements heavier than helium

Until now, no white dwarf has shown reliable evidence for the accretion of water-rich, rocky planetary material. Unambiguous signatures of icy asteroids at white dwarfs should include: 1) atmospheric metal pollution rich in refractory elements; 2) trace oxygen in excess of that expected for metal oxides; 3) circumstellar debris from which these elements are accreted, and, where applicable; 4) trace hydrogen (in a helium-dominated atmosphere) sufficient to account for the excess oxygen as H<sub>2</sub>O. Critically, the presence of a circumstellar disk signals that accretion is ongoing, identifies the source material, enables a confident, quantitative assessment of the accreted elemental abundances, and thus a calculation of the water fraction of the disrupted parent body.

The metal-enriched white dwarfs GD 362 and GD 16 both have circumstellar disks and relatively large, trace hydrogen abundances in helium-dominated atmospheres (21), but as yet no available assessment of photospheric oxygen (20, 22). These two stars have effective temperatures below 12 000 K and their trace hydrogen could potentially be the result of helium dredge-up in a previously hydrogen-rich atmosphere (23). The warmer, metal-lined white dwarfs GD 61 and GD 378 have photospheric oxygen (24), but the accretion history of GD 378 is unconstrained (i.e. it does not have a detectable disk), and without this information, the atmospheric oxygen could be consistent with that contained in dry minerals common in the inner Solar System (25). In the case of GD 61, elemental abundance uncertainties have previously prevented a formally significant detection of oxygen excess (26).

We obtained ultraviolet spectroscopy with the Cosmic Origins Spectrograph (COS) on board the *Hubble Space Telescope* of the white dwarf GD 61, and together with supporting ground-based observations, derived detections or limits for all the major rock-forming elements (O, Mg, Al, Si, Ca, Fe). These data permit a confident evaluation of the total oxygen fraction present in common silicates within the parent body of the infalling material, and we identify excess oxygen due to H<sub>2</sub>O as follows. 1) The observed carbon deficiency indicates that this element

has no impact on the total oxygen budget, even if every atom is delivered as  $\text{CO}_2$ . 2) The elements Mg, Al, Si, and Ca are assumed to be carried as  $\text{MgO}$ ,  $\text{Al}_2\text{O}_3$ ,  $\text{SiO}_2$ , and  $\text{CaO}$  at the measured or upper limit abundance. 3) The remaining oxygen exceeds that which can be bound in  $\text{FeO}$ , and the debris is interpreted to be water-rich. We find oxygen in excess of that expected for anhydrous minerals in the material at an  $\text{H}_2\text{O}$  mass fraction of 0.26 (Table 1, Fig. 1).

Because we have assumed the maximum allowed  $\text{FeO}$ , and some fraction of metallic iron is possible, the inferred water fraction of the debris is actually bound between 0.26 and 0.28. Although this makes little difference in the case of GD 61, where the parent body material appears distinctly mantle-like (26), there are at least two cases where metallic iron is a major (and even dominant) mass carrier within the parent bodies of circumstellar debris observed at white dwarfs (27). Overall, these data strongly suggest the material observed in and around polluted white dwarfs had an origin in relatively massive and differentiated planetary bodies.

We have assumed a steady state between accretion and diffusion in GD 61. However, a typical metal sinking timescale for this star is  $10^5$  yr, and thus the infalling disk material could potentially be in an early phase of accretion where material accumulates in the outer layers, prior to appreciable sinking (26). In this early phase scenario, the oxygen excess and water fraction would increase relative to those derived from the steady state assumption, and hence we confidently conclude that the debris around GD 61 originated in a water-rich parent body. Although the lifetimes of disks at white dwarfs are not robustly constrained, the best estimates imply that the chance of catching GD 61 in an early phase is less than 1% (16, 28, 29, 30).

The helium-rich nature of GD 61 permits an assessment of its trace hydrogen content and total asteroid mass for a single parent body. The total metal mass within the stellar convection zone is  $1.3 \times 10^{21}$  g, and roughly equivalent to a 90 km diameter asteroid. However, because metals continuously sink, it is expected that the destroyed parent body was substantially more massive, unless the star is being observed shortly after the disruption event. In contrast, hy-

drogen floats and accumulates, and thus places an upper limit on the total mass of accreted, water-rich debris. If all the trace hydrogen were delivered as H<sub>2</sub>O from a single planetesimal, the total accreted water mass would be  $5.2 \times 10^{22}$  g, and a 26% H<sub>2</sub>O mass fraction would imply a parent body mass of  $2 \times 10^{23}$  g, which is similar to that of the main belt asteroid 4 Vesta (31).

Based on these data, it appears that water in planetesimals can survive post-main sequence evolution. One possibility is that solid or liquid water is retained beneath the surface of a sufficiently large ( $d > 100$  km) parent body (25), and is thus protected from heating and vaporization by the outermost layers. Upon shattering during a close approach with a white dwarf, any exposed water ice (and volatiles) should rapidly sublimate but will eventually fall onto the star – the feeble luminosity of white dwarfs is incapable of removing even light gases by radiation pressure (30). Another possibility is that a significant mass of water is contained in hydrated minerals (e.g. phyllosilicates), as observed in main-belt asteroids via spectroscopy and inferred from the analysis of meteorites (32). In this case, the H<sub>2</sub>O equivalent is not removed until much higher temperatures and such water-bearing asteroids may remain essentially unaffected by the giant phases of the host star.

The white dwarf GD 61 contains the unmistakable signature of a rocky minor planet analogous to Ceres in water content (33), and probably analogous to Vesta in mass. The absence of detectable carbon indicates the parent body of the circumstellar debris was not an icy planetesimal analogous to comets, but instead similar in overall composition to asteroids in the outer main belt. This exoplanetary system originated around an early A-type star that formed large planetesimals similar to those found in the inner Solar System and which are the building blocks for Earth and other terrestrial planets.

## References and Notes

1. N. M. Batalha, *et al.*, *Astrophys. J.* **729**, 27 (2011)

2. F. Fressin, *et al.*, *Nature* **482**, 195 (2012)
3. D. K. Sing, *et al.*, *Mon. Not. R. Ast. Soc.* **416**, 1443 (2011)
4. C. M. Lisse, *et al.*, *Astrophys. J.* **747**, 93 (2012)
5. D. Koester, *Astron. Astrophys.* **498**, 517 (2009)
6. B. Zuckerman, D. Koester, I. N.Reid, M. Hünsch, *Astrophys. J.* **596**, 477 (2003)
7. D. Koester, D. Wilken, *Astron. Astrophys.* **453**, 1051 (2006)
8. J. Farihi, M. A. Barstow, S. Redfield, P. Dufour, N. C. Hambly, *Mon. Not. R. Ast. Soc.* **404**, 2123 (2010)
9. M. Jura, J. Farihi, B. Zuckerman, *Astron. J.* **137**, 3191 (2009)
10. W. T. Reach, M. J. Kuchner, T. von Hippel, A. Burrows, F. Mullally, M. Kilic, D. E. Winget, *Astrophys. J.* **635**, L161 (2005)
11. B. T. Gänsicke, T. R. Marsh, J. Southworth, A. Rebassa-Mansergas, *Science* **314**, 1908 (2006)
12. J. H. Debes, K. J. Walsh, Kevin J., C. Stark, *Astrophys. J.* **747**, 148 (2012)
13. J. Farihi, B. T. Gänsicke, P. R. Steele, J. Girven, M. R. Burleigh, E. Breedt, D. Koester, *Mon. Not. R. Ast. Soc.* **421**, 1635 (2012)
14. J. Farihi, M. Jura, J. E. Lee, B. Zuckerman, *Astrophys. J.* **714**, 1386 (2010)
15. S. Xu, M. Jura, *Astrophys. J.* **745**, 88 (2012)
16. J. Girven, C. S. Brinkworth, J. Farihi, B. T. Gänsicke, D. W. Hoard, T. R. Marsh D. Koester, *Astrophys. J.* **749**, 154 (2012)

17. J. Farihi, M. Jura, B. Zuckerman, *Astrophys. J.* **694**, 805 (2009)
18. M. Jura, J. Farihi, B. Zuckerman, *Astrophys. J.* **663**, 1285 (2007)
19. M. Jura, *Astrophys. J.* **584**, L91 (2003)
20. B. Zuckerman, D. Koester, C. Melis, B. M. S. Hansen, M. Jura, *Astrophys. J.* **671**, 872 (2007)
21. M. Jura, M. Muno, J. Farihi, B. Zuckerman, *Astrophys. J.* **699**, 1473 (2009)
22. D. Koester, R. Napiwotzki, B. Voss, D. Homeier, D. Reimers, *Astron. Astrophys.* **439**, 317 (2005)
23. P. E. Tremblay, P. Bergeron, *Astrophys. J.* **672**, 1144 (2008)
24. S. Desharnais, F. Wesemael, P. Chayer, J. W. Kruk, R. A. Saffer, *Astrophys. J.* **672**, 540 (2008)
25. M. Jura, S. Xu, *Astron. J.* **140**, 1129 (2010)
26. J. Farihi, C. S. Brinkworth, B. T. Gänsicke, J. Girven, T. R. Marsh, D. W. Hoard, B. Klein, D. Koester, *Astrophys. J.* **728**, L8 (2011)
27. B. T. Gänsicke, D. Koester, J. Farihi, J. Girven, S. G. Parsons, E. Breedt, 2012, *Mon. Not. R. Ast. Soc.* **424**, 333
28. B. Klein B., M. Jura, D. Koester, B. Zuckerman, C. Melis, *Astrophys. J.* **709**, 950 (2010)
29. M. Jura, *Astron. J.* **135**, 1785 (2008)
30. J. Farihi, B. Zuckerman, E. E. Becklin, *Astrophys. J.* **674**, 421 (2008)
31. C. T. Russell, *et al.*, *Science* **336**, 684 (2012)

32. A. S. Rivkin, E. S. Howell, F. Vilas, L. A. Lebofsky, in Asteroids III, W. F. Bottke Jr., A. Cellino, P. Paolicchi, R. P. Binzel Eds. (University of Arizona Press, Tucson), p.235-253
33. P. C. Thomas, *Nature* **437**, 224 (2005)
34. C. Visscher, B. Fegley, Jr., *Astrophys. J.* **767**, L12 (2013)
35. A. I. Sheinis, M. Bolte, H. W. Epps, R. I. Kibrick, J. S. Miller, M. V. Radovan, B. C. Bigelow, B. M. Sutin, *Proc. Astron. Soc. Pacific*, **114**, 851 (2002)
36. D. Koester, *Memorie della Societa Astronomica Italiana*, **81**, 921 (2010)

This work is based on observations made with the *Hubble Space Telescope* which is operated by the Association of Universities for Research in Astronomy under NASA contract NAS 5-26555. These observations are associated with program 12474. Some of the data presented herein were obtained at the W.M. Keck Observatory, which is operated as a scientific partnership among the California Institute of Technology, the University of California and the National Aeronautics and Space Administration. The Observatory was made possible by the generous financial support of the W.M. Keck Foundation. Keck telescope time for program 2011B-0554 was granted by NOAO through the Telescope System Instrumentation Program, funded by NSF. J. Farihi acknowledges support from the United Kingdom Science and Technology Facilities Council in the form of an Ernest Rutherford Fellowship (ST/J003344/1). The research leading to these results has received funding from the European Research Council under the European Union's Seventh Framework Programme (FP/2007-2013) / ERC Grant Agreement no. 320964 (WDTracer). B.T. Gänsicke was supported in part by the UK Science and Technology Facilities Council (ST/I001719/1).

Table 1: Oxide and Water Mass Fractions in the Planetary Debris at GD 61

Oxygen Carrier	Steady State	Early Phase
CO <sub>2</sub>	< 0.002	< 0.002
MgO	0.17	0.18
Al <sub>2</sub> O <sub>3</sub>	< 0.02	< 0.02
SiO <sub>2</sub>	0.32	0.27
CaO	0.02	0.01
FeO <sup>a</sup>	0.05	0.02
Excess	0.42	0.50
H <sub>2</sub> O in debris:	0.26	0.33

*Note.* We adopt the steady state values which assume accretion-diffusion equilibrium.

<sup>a</sup> All iron is assumed to be contained in FeO, while some metallic Fe will modestly increase the excess oxygen.

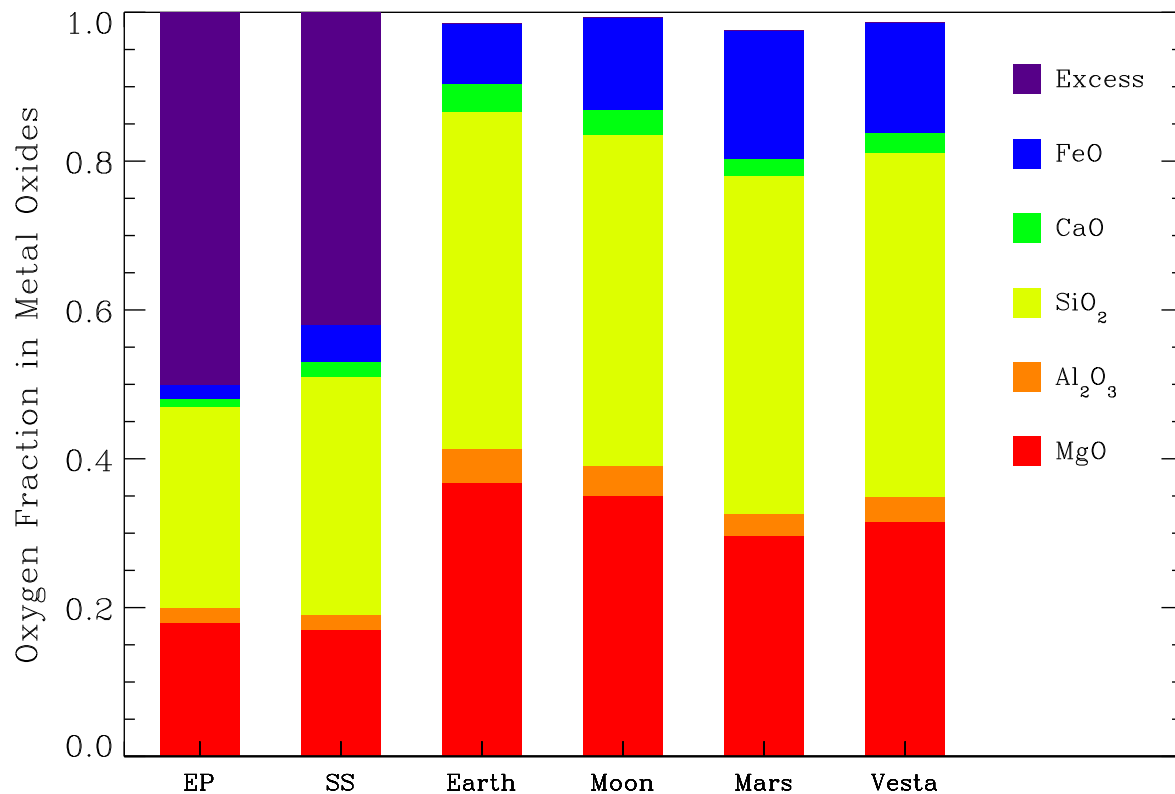


Figure 1: The first two columns are the early phase (EP) and steady state (SS) fractions of oxygen carried by all the major rock-forming elements in GD 61, assuming all iron is carried as FeO. Additional columns show the oxide compositions of the bulk silicate (crust plus mantle) Earth, Mars, Moon, and Vesta (34). Their totals do not reach 1.0 as trace oxides have been omitted. The overall chemistry of GD 61 is consistent with a body composed almost entirely of silicates, and thus appears relatively mantle-like, but with significant water. In contrast, the Earth is relatively water poor and contains approximately 0.023% H<sub>2</sub>O ( $1.4 \times 10^{24}$  g).

# *Supporting Online Material for* Evidence for Water in the Rocky Debris of a Disrupted Extrasolar Minor Planet

We describe here in detail the observations and analyses supporting the main paper, specifically the spectroscopy of the metal-enriched, white dwarf atmosphere and the analytical link to the elemental abundances of the infalling planetary debris.

## **Summary of the Observations and Datasets**

GD 61 exhibits infrared excess consistent with circumstellar dust orbiting within its Roche limit (26), and bears the unambiguous signature of debris accretion via its metal-polluted atmosphere.

The white dwarf was observed with the Cosmic Origins Spectrograph (COS) during *Hubble Space Telescope* Cycle 19 on 2012 January 28. The ultraviolet spectra were obtained with a total exposure time of 1600 s (split between two FP-POS positions) using the G130M grating and a central wavelength setting at 1291 Å, covering 1130–1435 Å at  $R \approx 18\,000$ . The COS data were processed and calibrated with CALCOS 2.15.6, and are shown in Figure 2. Optical spectroscopy of GD 61 was obtained on 2011 October 24 with the Keck II Telescope and the Echelle Spectrograph and Imager (35, *ESI*) in echelle mode, effectively covering 3900–9200 Å at  $R \approx 13\,000$ . The spectra were obtained in a series of 16 exposures of 900 s each, for a total exposure time of 4 hr, and reduced using standard tasks in IRAF<sup>2</sup>.

---

<sup>2</sup>IRAF is distributed by the National Optical Astronomy Observatories, which are operated by the Association of Universities for Research in Astronomy, Inc., under cooperative agreement with the National Science Foundation.

## Derivation of Photospheric and Debris Abundances

Elemental abundances for GD 61 were derived from the COS and ESI data by fitting white dwarf atmospheric models (36) to the observed spectra. For these calculations,  $T_{\text{eff}} = 17\,280\text{ K}$  and  $\log g = 8.20$  are adopted, based on a published analysis of low-resolution optical spectra (24). The resulting photospheric abundances and upper limits are listed in Table 2 together with previous measurements from the *Far Ultraviolet Spectroscopic Explorer* (24, *FUSE*) and Keck I HIRES (26). Notably, all heavy element abundances agree well, despite being derived using separate instruments and with multiple absorption lines across distinct wavelength regimes.

The transformation between the heavy element abundances in the white dwarf atmosphere and those within the infalling planetary debris are calculated assuming a steady state balance between accretion and diffusion. An early (or build-up) phase of accretion is theoretically possible in GD 61, but this is unlikely (see main paper). Importantly, in this case an early phase would imply a larger oxygen excess and  $\text{H}_2\text{O}$  fraction, and therefore the more conservative, and most probable, assumption is made.

For white dwarfs with significant convection zones like GD 61, the atmospheric mass fraction  $X_z$  of heavy element  $z$  is related to its accretion rate  $\dot{M}_z$  via

$$\dot{M}_z = X_z M_{\text{cvz}} / t_z \quad (1)$$

where  $t_z$  is the sinking timescale for the element and  $M_{\text{cvz}}$  is the mass of the stellar convection zone. The mass fraction is determined from the model atmosphere fits and the sinking timescale is known from white dwarf diffusion calculations (5). In essence, Equation S1 states that the accretion rate of element  $z$  equals its rate of depletion as it settles below the mixing layer. The ratio of two heavy elements within the debris (and hence parent body) is either the ratio of their respective accretion rates in the steady state, or the ratio of their atmospheric mass fractions in

the early phase, and related by

$$\frac{\dot{M}_{z1}}{\dot{M}_{z2}} = \frac{X_{z1}}{X_{z2}} \times \frac{t_{z2}}{t_{z1}} \quad (2)$$

Table 3 lists the relevant quantities of GD 61 for the key elements that determine the total oxygen budget of the debris. The steady state metal abundances relative to oxygen are taken from the fourth column. The sinking timescales for GD 61 have been updated following a correction in the theoretical calculations<sup>3</sup>, and they are somewhat different than those presented in a previous analysis (26). Notably, this correction has strengthened the case for an oxygen excess in GD 61.

## Evaluation of Oxygen Excess and Uncertainties

The method for calculating the overall oxygen budget is as follows. We begin with the columns in Table 3, and in particular we identify the total oxygen budget with: 1) its mass accretion rate for the steady state or 2) its mass within the stellar convection zone for the early phase. We calculate the fraction of oxygen that can be absorbed as CO<sub>2</sub> based on the upper limit for carbon, and subtract this from the total available. Next, we perform a similar calculation for the mass of oxygen in MgO, Al<sub>2</sub>O<sub>3</sub>, SiO<sub>2</sub>, CaO, and FeO based on their detections or upper limits, again subtracting these from the budget. After accounting for all the major oxygen carriers, any remaining mass is considered excess.

The collective data for GD 61 are robust and comprehensive, comprising four instruments with each probing distinct wavelength regions and containing multiple transitions for each element from the far-ultraviolet to the red optical region. The uncertainties in the metal abundances of this white dwarf are given as  $3\sigma$  adopted values in the last column of Table 2. Using a brute force approach, all 128 possible combinations of abundance values are calculated for C, O, Mg, Al, Si, Ca, Fe where the abundances  $N(X)/N(\text{He})$  take on each of the values  $x \pm \delta x$ . Evaluating

---

<sup>3</sup><http://www1.astrophysik.uni-kiel.de/~koester/astrophysics/astrophysics.html>

all possible permutations, the dispersion in the resulting oxygen excess values (0.068) results in a  $6.1\sigma$  confidence for the case of steady state accretion.

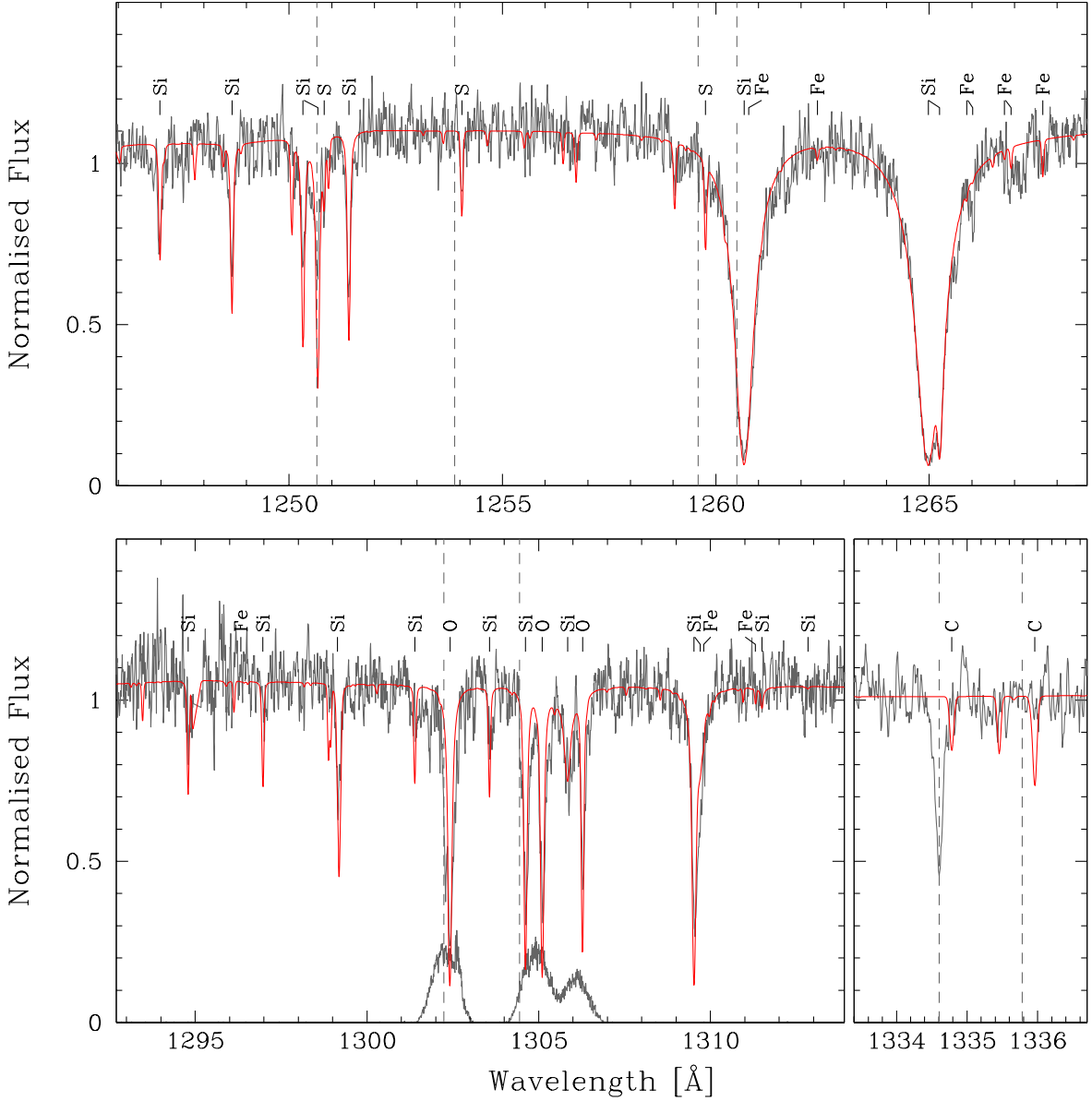


Figure 2: The normalized COS spectra of GD 61 (grey), together with the best fitting model spectra (red). Interstellar absorption features are indicated by vertical grey dashed lines, and are blueshifted with respect to the photospheric features by  $40 \text{ km s}^{-1}$ . Geocoronal airglow of O I at  $1302.2$ ,  $1304.9$ , and  $1306.0 \text{ \AA}$  can contaminate COS spectra to some degree, and typical airglow line profiles are shown in the middle panel scaled to an arbitrary flux.

Table 2: Elemental Abundances  $N(X)/N(\text{He})$  in GD 61

Element	Ultraviolet		Optical		Adopted
	COS	FUSE	ESI	HIRES	
Detections:					
H	-3.70 (0.10)		-4.00 (0.10)	-3.98 (0.10)	-3.89 (0.15)
O	-6.00 (0.15)	-5.80 (0.20)	-5.75 (0.20)		-5.95 (0.13)
Mg	-6.50 (0.30)		-6.74 (0.10)	-6.65 (0.18)	-6.69 (0.14)
Si	-6.82 (0.12)	-6.70 (0.20)	-6.85 (0.10)	-6.85 (0.09)	-6.82 (0.11)
S	-8.00 (0.20)				-8.00 (0.20)
Ca			-7.77 (0.06)	-7.90 (0.19)	-7.90 (0.19)
Fe	-7.60 (0.30)	-7.60 (0.20)			-7.60 (0.20)
Upper limits:					
C	-9.10	-8.80			
N	-8.00				
Na			-6.80		
P	-8.70				
Al	-7.80			-7.20	
Ti	-8.60				
Sc	-8.20				
Cr	-8.00				
Fe				-7.50	
Ni	-8.80				

Table 3: Atmospheric and Debris Properties for Key Trace Elements in GD 61

Element	$t_{\text{diff}}$ ( $10^5$ yr)	Early Phase	Steady State
		$X_z M_{\text{cvz}}^a$ ( $10^{21}$ g)	$\dot{M}_z$ ( $10^8$ g s $^{-1}$ )
H	$\infty$	5.755	
C	1.730	< 0.001	< 0.001
O	1.706	0.802	1.489
Mg	1.808	0.222	0.389
Al	1.735	< 0.019	< 0.035
Si	1.438	0.190	0.419
S	0.952	0.014	0.048
Ca	0.782	0.023	0.091
Fe	0.855	0.063	0.232
Total Z		1.332	2.704

*Note.* The metal-to-metal ratios within the planetary debris for the early phase and steady state regimes are derived directly from the values in the third and fourth columns respectively.

<sup>a</sup>The third column is the mass of each element residing in the convection zone of GD 61, and their total (excluding hydrogen) represents a minimum mass for the parent body due to the continual sinking of metals.